ELSEVIER

PII: S0032-3861(97)10114-8

Polymer Vol. 39 No. 21, pp. 5183–5195, 1998
0032-3861/98/$ – see front matter

Sorptive dilation and relaxational processes in glassy polymer/gas systems—I. Poly(sulfone) and poly(ether sulfone)

M. Böhning and J. Springer*
Technische Universität Berlin, Institut für Technische Chemie, Fachgebiet Makromolekulare Chemie, Straße des 17. Juni 135, D-10623 Berlin, Germany
(Received 30 July 1997; accepted 4 September 1997)

The volumetric behaviour of glassy poly(sulfone) and poly(ether sulfone) under gas pressures of CO_2, N_2O and CH_4 up to 50 bar was investigated at 35°C using a new experimental technique based on a capacitive distance measurement. Corresponding gas concentrations within the polymers were determined by gravimetric gas sorption measurements. The time-dependent dilation after a pressurising step reveals two distinct dilation modes. The analysis of the first dilation mode according to mass transport kinetics is in good agreement with diffusion coefficients from time-lag experiments, whereas the slower secondary process has to be considered as volume relaxation resulting from the enhanced polymer chain mobility and the stress exerted by the sorbed gas molecules.

(Keywords: gas sorption; dilation; volume relaxation)

INTRODUCTION

The sorption and transport behaviour of gases is an important issue with regard to the application of polymers as barrier materials for coatings and packaging[1] as well as for gas separation membranes[2–4].

The mass transport of low molecular weight substances in non-porous polymeric membranes is generally described in terms of a solution-diffusion process consisting of three steps: (1) sorption of the penetrant molecules at the side of higher chemical potential (i.e. the high-pressure or 'upstream' side); (2) diffusive transport through the polymer matrix; (3) desorption at the side of lower chemical potential (i.e. the low-pressure or 'downstream' side). The transport is directed along the gradient of the chemical potential determined by the concentrations at the upstream and downstream boundary of the membrane.

Therefore, in most cases the starting point of the description of the gas transport in polymers is the sorption behaviour for which several models have been proposed[5,6]. For glassy polymers exhibiting a characteristic decrease of gas solubility with increasing pressure, some of these models are based on the assumption of two distinct sorption mechanisms (dual mode sorption)[7,8] or a continuous distribution of sorption site energies[9] and others are based primarily on the consideration of the influence of gas/polymer interactions on gas sorption[10,11].

In order to gain further insight into the sorption mechanisms involved and the influences of polymer properties, such as chain mobility and free volume, or plasticisation and conditioning effects several methods have been described to investigate the volumetric changes of the polymer matrix during the sorption of gas molecules[12–18]. Most of those approaches are based on the optical determination of the length-dilation of a polymer film placed in a pressurised view-cell[13–16,18]. Briscoe and Zakaria employ an ultrasonic technique to measure the distance between the polymer sample and the fixed sensor under gas pressure conditions[17].

The appearance of relaxational phenomena during dilation experiments has already been reported for several glassy polymers[18,19] and a qualitative model has been proposed for their description[18].

In our study we want to compare the influence of different gases on the volumetric behaviour of glassy poly(sulfone) as well as poly(ether sulfone). A new technique has been developed to determine the length-change of a polymer film under elevated gas pressures based on a capacitive distance measurement providing high accuracy and easy data acquisition by computer.

EXPERIMENTAL

Materials

For this study commercially available poly(arylene)s were used as melt extruded films of 100 μm thickness. For characterisation of the polymer samples thermal properties were examined using a differential scanning calorimeter (DSC) Perkin Elmer DSC-7 at 10 K/min. Densities were obtained from flotation in a density gradient column (DGT) with aqueous $Ca(NO_3)_2$ solution and calibrated glass floats at 23°C.

Poly(sulfone) (PSU, '*Ultrason S*') and Poly(ether sulfone) (PES, '*Ultrason E*') were obtained from BASF AG, Germany. For both polymers no indications for crystallinity or crystallisation were found in the DSC experiments.

All films were free of fillers or additives, which was proven by thermogravimetric analysis (TGA) using a Setaram B70 thermobalance. The structures of the polymers are shown in *Figure 1*. Glass transition temperatures and densities are given in *Table 1*. The gases, carbon dioxide, nitrous oxide and methane, were received from

* To whom correspondence should be addressed

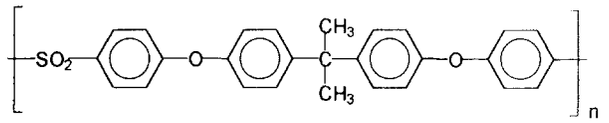

Poly(sulfone)

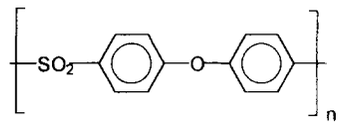

Poly(ether sulfone)

Figure 1 Structures of the two poly(arylene)s used in this study

Table 1 Glass transition temperatures and densities of the poly(arylene)s used in this study

Polymer	T_G	ρ
	/°C	/g/cm^3
Poly(sulfone) (PSU)	187	1.237
Poly(ether sulfone) (PES)	227	1.337

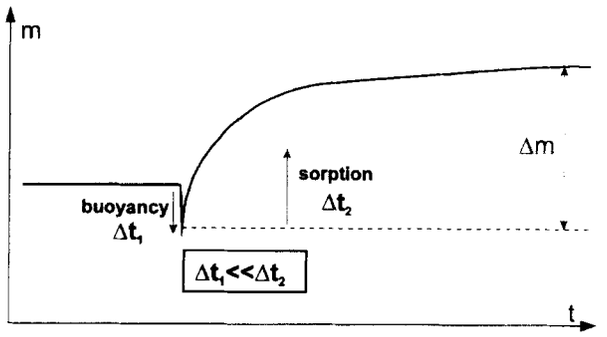

Figure 2 Schematic representation of an experimental sorption step

Messer-Griesheim, Germany, with purities > 99.99% and 99.5%, respectively.

Sorption

The concentration of sorbed penetrant was measured gravimetrically using an electronic high-pressure microbalance equipped with a vacuum pump and gas supply system which has been described earlier[20]. Compared with Ref. [20] an improved temperature control system using a self-optimising PID-controller and direct heating of the air bath containing the whole pressure-chamber with the microbalance, valves and tubing, has been added to the sorption apparatus. Hereby the perturbations of the weighing-system resulting from temperature gradients and convective gas flow have been further reduced. Alternatively, an equivalent system for gas sorption measurements has been integrated in the gas-pressure dilatometer described below.

After degassing the sample within the sorption balance for at least 48 h under vacuum ($< 10^{-4}$ mbar) the gas pressure was increased stepwise and mass change was recorded for each step. The mass change connected with the occurrence of buoyancy forces could be separated due to their immediate effect compared with the significantly slower kinetic of the gas sorption, which is determined by the diffusion of the gas molecules (*Figure 2*).

The mass uptake after the n^{th} pressure step is given by the sum of mass increments Δm:

$$m_{\text{gas},n} = \sum_{i=0}^{n} \Delta m_i. \tag{1}$$

The concentration C of the sorbed penetrant gas, given in cm^3(STP)/cm^3(polymer), is then calculated from the mass uptake m_{gas} using equation (2), where R is the gas constant, $T_0 = 273.15$ K, $p_0 = 1.013$ bar, ρ_{polymer} is the density and m_{polymer} is the mass of the polymer sample and M_{gas} is the molar mass of the sorbed gas.

$$C = \left[\frac{R \cdot T_0}{P_0} \cdot \frac{\rho_{\text{polymer}}}{m_{\text{polymer}} \cdot M_{\text{gas}}}\right] \cdot m_{\text{gas}} \tag{2}$$

Dilation

For our studies of the dilation behaviour of polymers under elevated gas pressures, a new apparatus based on a capacitive distance measurement system (*capa-NCDT*, Micro-Epsilon Meßtechnik, Ortenburg, Germany) was designed and constructed. The distance measurement is contactless and the resolution of the sensor used in our set-up is > 0.05 μm within a distance range of 1 mm. After signal processing the resulting resolution at the computer interface is 0.5 μm, which is mainly determined by the built-in A/D-converter of the system[21].

The sensor is fixed in the lower plate of the sample holder with the polymer film sample suspended above it (*Figure 3*). The sample is clamped between two thin brass holders with

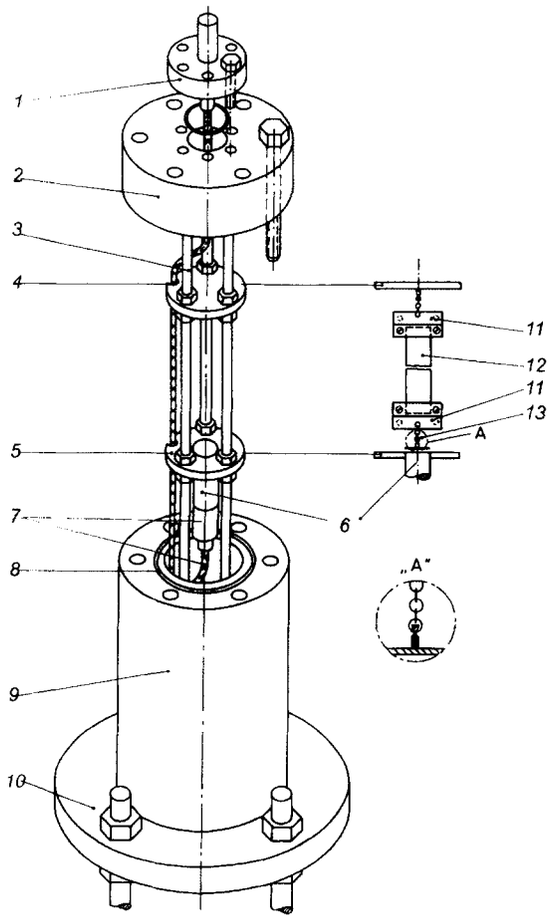

Figure 3 Gas-pressure dilatometer (GPD): 1, triaxial electrical feed-through; 2, top cover; 3, metal rods with thread (M4); 4/5, sample holder – upper/lower plate; 6, sensor; 7, sensor cabling; 8, o-ring sealing; 9, stainless steel autoclave; 10, metal rods with thread (M8); 11, polymer film holder; 12, sample; 13, attached counter electrode

a perpendicular metal electrode attached at the lower end. The metal electrode is aligned parallel to the sensor surface and changes of the distance between sensor surface and electrode represent changes of the sample length.

The sample holder is attached to the o-ring sealed top cover of a stainless steel autoclave allowing pressurisation up to 70 bar. The upper and lower plates of the sample holder are variable in height and allow adaption to different sample lengths ($l_0 = 1-8$ cm). The autoclave and the sample holder of the gas-pressure dilatometer are shown in *Figure 3*.

The sensor is connected to the pre-amplifier of the measuring system using a triaxial electrical vacuum-feedthrough (Vermetal, France). The characteristics of the modified sensor cable were taken into account by separate calibration measurements, as well as the influence of the dielectric constant ϵ_r, which changes with pressure and the type of gas. For these calibration measurements the sample holder was replaced by a micrometer and different fixed distances between sensor and opposite electrode could be set and measured. To make the ϵ_r-dependent calibration for different gases and pressures easier, a second sensor with a fixed opposite electrode is placed within the pressurised autoclave and connected to the second channel of the distance–measurement system.

A scheme of the set-up for the gas-pressure dilatometric experiments is shown in *Figure 4*. It consists of the gas-pressure dilatometer (C) described above, a high-pressure microbalance (Sartorius 4406) (D), an additional autoclave (B) for easier pressure adjustment, temperature control unit and vacuum system. The high-pressure microbalance allows the measurement of the gas sorption parallel to the gas-pressure dilatometric investigations.

Both systems and all valves and tubing are placed within a closed housing in which an air-bath temperature control was realised using a self-optimising PID-controller (Eurotherm 818S) with electrical heating elements and a constant cooler with a heat-exchanger on the inside of the housing.

For data acquisition a PC was used, which also recorded values of gas pressure as well as the temperatures of the air-bath and the dilatometer pressure chamber. Prior to analysis the recorded distance values (d') were corrected according to the previously determined calibration factors considering the pressure-dependent dielectric constant ϵ_r and electrical characteristics of the sensor cabling.

After degassing of the sample gas-pressure dilatometric experiments were conducted by stepwise increases of the gas pressure to obtain isotherms analogous to the sorption measurements.

A typical curve of the uncorrected distance signal d' is shown in *Figure 5*. The sampling rate was 10 s for all experiments presented in this study. After increasing the pressure an apparent change of the distance signal occurs instantaneously due to the change of the dielectric constant $\Delta\epsilon_r$ of the gas phase. Then a continuous decrease of the measured distance approaching a new equilibrium value is observed as a result of the elongation of the polymer film sample due to sorptive dilation.

Assuming isotropic swelling of the polymer which has been proven for two dimensions by test measurements with film sample orientations turned by 90°, the volume change can be calculated according to equation (3) from the elongation ($\Delta L/L_0$) observed experimentally.

$$\left(\frac{\Delta V}{V_0}\right) = \left(\frac{L}{L_0}\right)^3 - 1 = \left(1 + \frac{\Delta L}{L_0}\right)^3 - 1 \qquad (3)$$

L_0 and V_0 are the initial length and volume of the sample

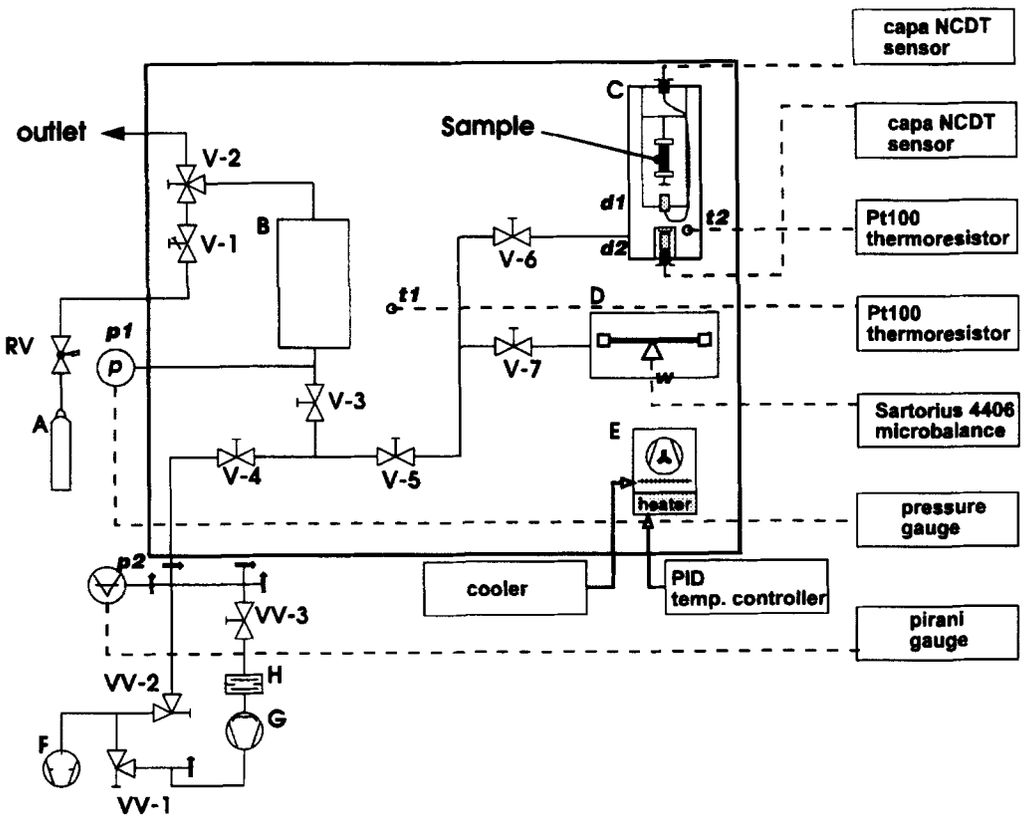

Figure 4 Scheme of the experimental set-up for gas-pressure dilatometric measurements (V-1–V-7, valves; VV-1–VV-3, vacuum valves; RV, pressure reducing valve; A, gas bomb; B, autoclave; C, gas-pressure dilatometer (GPD); D, high-pressure microbalance; E, heat exchanger with fan; F, rotating vacuum pump; G,H, oil diffusion vacuum pump with baffle; d1, length sensor/sample; d2, length sensor/reference; t1, Pt100 thermosensor/air-bath; t2, Pt100 thermosensor/GPD; p1, piezoresistive pressure gauge (1–100 bar); p2, pirani vacuum gauge)

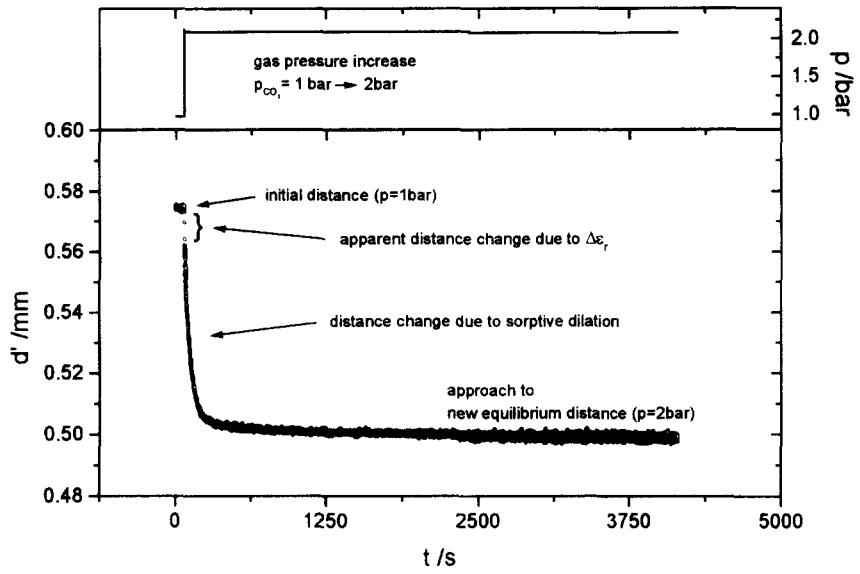

Figure 5 Uncorrected distance signal d' after increasing the system pressure

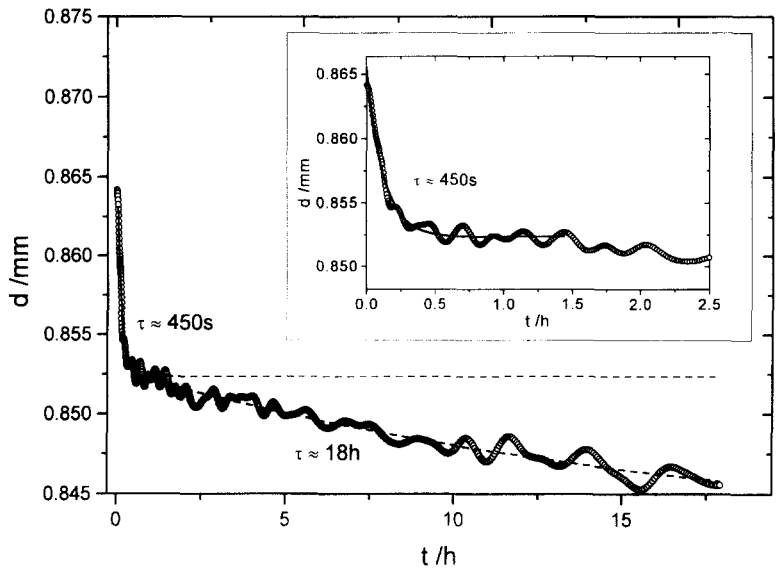

Figure 6 Corrected experimental distance curve for a short (inset) and a long observation time (PES/CO_2/16 bar/35°C, τ-time constants from exponential fit)

after degassing. The partial molar volume (PMV) of the gas sorbed in the polymer

$$\bar{V}_{m,\mathrm{gas}} = \left(\frac{\partial V}{\partial n_{\mathrm{gas}}}\right)_{T,n_{\mathrm{polymer}}} \tag{4}$$

can be calculated from the volume change with increasing concentration C according to equation (5), where $V^0_{m,\mathrm{gas}}$ is the molar volume of the ideal gas under STP conditions (22 400 cm^3/mol).

$$\bar{V}_{m,\mathrm{gas}} = \frac{V^0_{m,\mathrm{gas}}}{V_0}\cdot\left(\frac{\partial V}{\partial C}\right)_T = V^0_{m,\mathrm{gas}}\cdot\left(\frac{\partial (V/V_0)}{\partial C}\right)_T \tag{5}$$

The PMV of the gas is determined from the slope of $(V/V_0)_T$ or $(\Delta V/V_0)_T$ plotted against the gas concentration C.

RESULTS AND DISCUSSION

Dilation measurement and analysis

For low gas pressures or short observation times under higher gas pressures the recorded distance signal approaches a new equilibrium value, as indicated in *Figure 5* within a few hours. After longer times, especially at higher gas concentrations, another secondary change of the sample length was observed also approaching a constant value. This behaviour is shown in *Figure 6* by way of example for PES at 16 bar CO_2 pressure.

The rate of the two distinct dilation processes can be estimated from the time constants τ of exponentials fitted to the experimental values within the different time ranges (see *Figure 6*).

An analysis of the mass transport kinetics obtained by plotting the distance ratio $(\Delta d_t/\Delta d_\infty)$ against $\sqrt{t}/l^2$ (*Figure 7*), where l is the thickness of the film sample and Δd_∞ is taken from the first plateau of the distance curve, shows good agreement with gas transport data obtained using the time-lag technique[22] described earlier[23]. From the half-time analysis of the curve in *Figure 7* according to equation (6)[22] a diffusion coefficient of $D = 1.28\cdot10^{-8}$ cm^2/s is calculated while the apparent diffusion coefficient from the time-lag

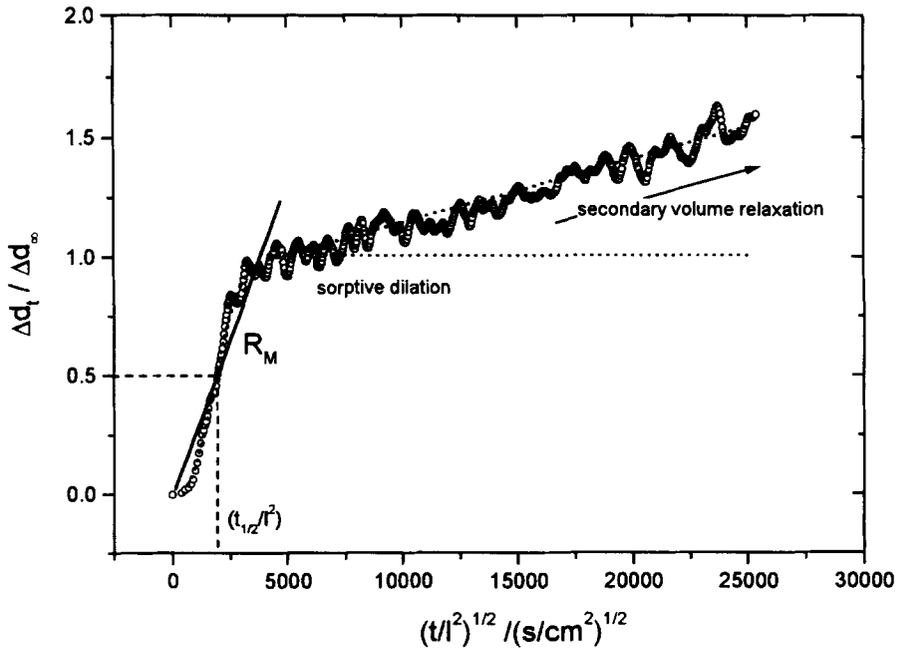

Figure 7 Analysis according to mass transport kinetics (PES/CO_2/16 bar/35°C)

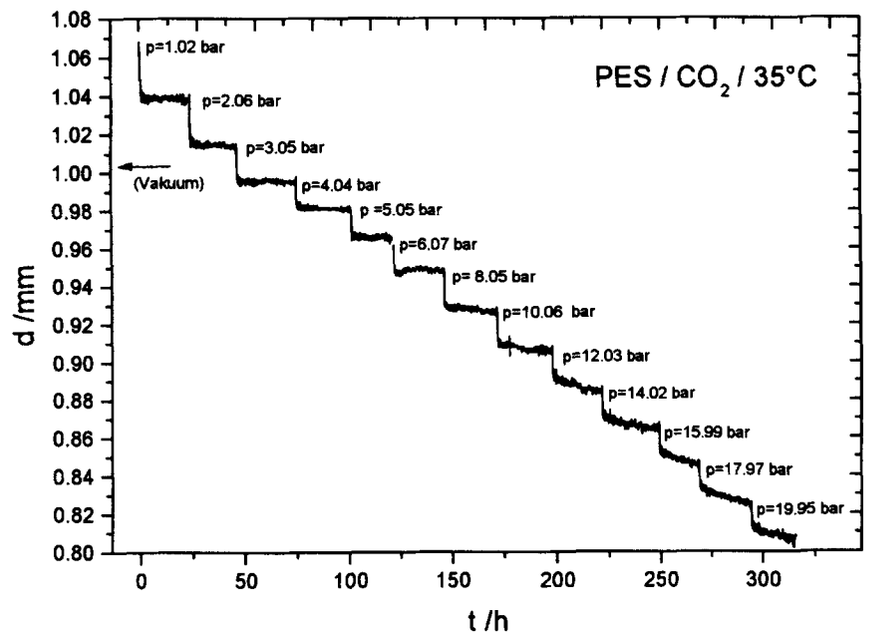

Figure 8 Experimental distance curves for pressure steps 1 to 13 (1–20 bar, PES/CO_2/35°C)

experiment at 15 bar CO_2 upstream pressure is $D_{app} = 1.19 \cdot 10^{-8}$ cm^2/s.

$$D \approx 0.049/\left(\frac{t_{1/2}}{l^2}\right) \quad (6)$$

The sigmoidal shape of the dilation curve in *Figure 7* is due to a delay of the dilation in comparison to the gas uptake. This delay corresponds to the time which is necessary to establish a gas concentration along the film thickness sufficient to cause the length-change of the whole sample[18].

From the slope R_M obtained from linear regression of the initial part of the experimental curve (solid line in *Figure 7*) a diffusion coefficient of $D = 1.27 \cdot 10^{-8}$ cm^2/s is calculated using equation (7)[22].

$$D = \frac{\pi}{16} \cdot R_M^2 \quad (7)$$

Thus, the overall initial stage of the dilation process is in good agreement with the sorption kinetics determined by the diffusivity of the penetrant molecules.

Therefore, it can be concluded that the first dilation process which follows the diffusion kinetics is directly connected with the sorption of the penetrant gas. The slower secondary dilation has to be considered as a volume relaxation resulting from changes of the polymer matrix due to gas/polymer interactions.

The primary dilation observed after the stepwise rising of gas pressure decreases with increasing pressure because of the decreasing solubility which is characteristic for glassy polymers, resulting in smaller amounts of gas sorbed during the individual pressure step. In contrast, the secondary dilation becomes more prominent due to the higher concentration of sorbed gas molecules being present in the polymer matrix under increasing pressure. This can be clearly seen from *Figure 8*, where the first 13 pressure steps for PES/CO_2 at 35°C are shown as an example.

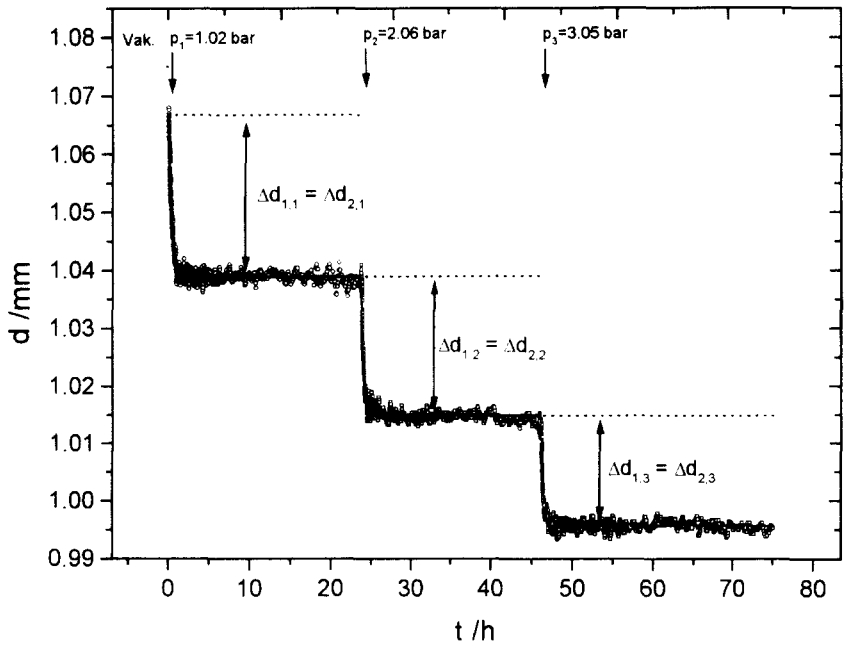

Figure 9 Experimental distance curves for pressure steps 1 to 3 (1–3 bar, PES/CO_2/35°C)

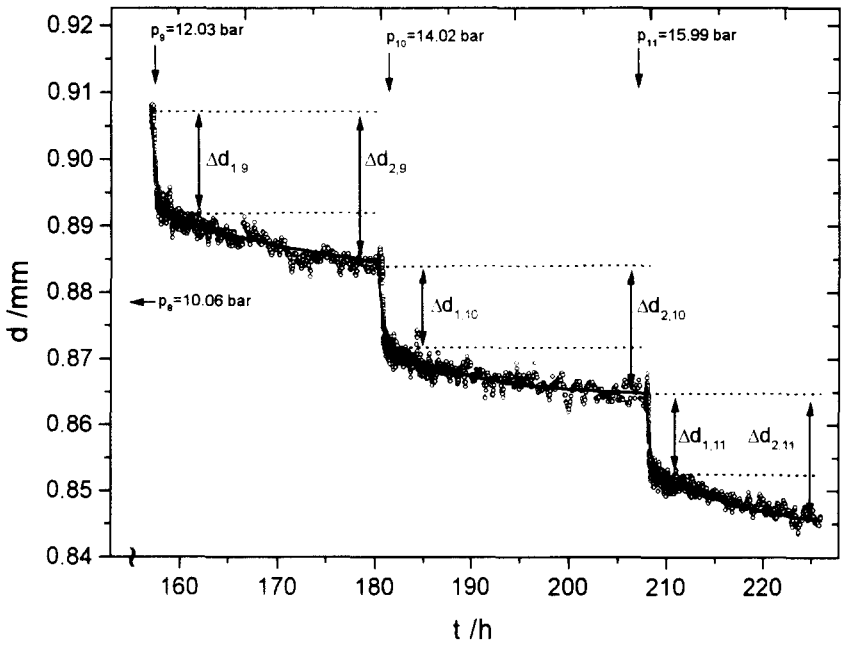

Figure 10 Experimental distance curves for pressure steps 9 to 11 (12– 16 bar, PES/CO_2/35°C)

As a consequence of the finding of two distinct dilation processes the analysis of the experimental data was divided into a short-time analysis covering the primary (directly sorptive) dilation process and a long-time analysis including also the secondary volume relaxation. The corresponding changes of the sample length are calculated according to equations (8) and (9) for the short-time and long-time analysis, respectively.

$$\Delta L_{1,n} = \sum_{i=1}^{n} \Delta d_{1,i} \tag{8}$$

$$\Delta L_{2,n} = \sum_{i=1}^{n} \Delta d_{2,i} \tag{9}$$

The difference of the distances $\Delta d_{1,i}$ and $\Delta d_{2,i}$ can be seen from *Figure 9*, where practically no secondary dilation occurs under low CO_2 pressures, and *Figure 10* with pronounced secondary dilation under higher CO_2 pressures. The corresponding volume dilations ($\Delta V_1/V_0$) and ($\Delta V_2/V_0$) were calculated according to equation (3).

It should be noted that the two resulting dilation isotherms are not measured independently. Therefore, the n^{th} dilation step could be influenced by all preceding pressure steps resulting in primary dilation as well as secondary volume relaxation.

The sorption isotherms measured for all polymer/gas pairs investigated by gas-pressure dilatometry exhibit the characteristic curvature concave to the pressure axis characteristic for glassy polymers. In order to calculate the

pressure-dependent gas concentrations needed for further analysis of the dilation isotherms a simple power-function with two parameters (b, c) (equation (10)) was used for interpolation instead of the usually employed sorption models (e.g. dual-mode sorption).

$$C = b \cdot p^c \tag{10}$$

The power-function was found empirically to provide a good description of the experimental sorption data and a good convergence behaviour during curve fitting. Subsequent sorption curves (except *Figure 11*, where experimental data points are also shown) are representations of the experimental data based on the fit-function used for interpolation with parameters given in the figure captions.

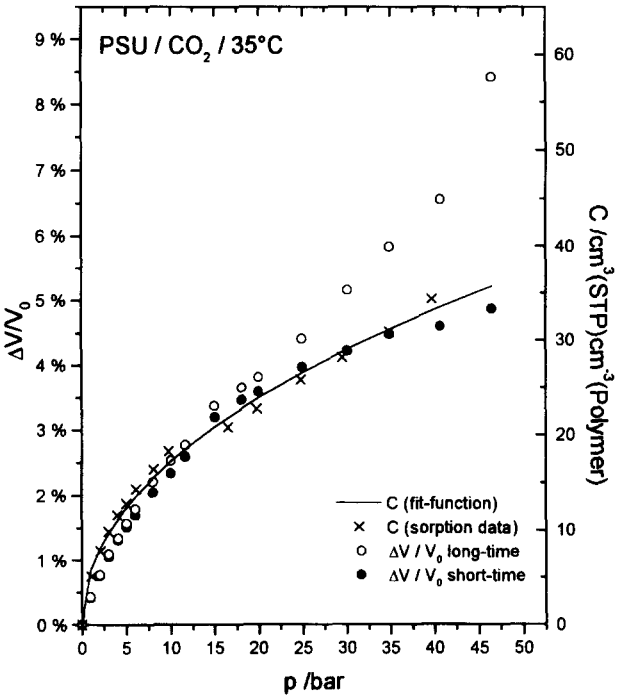

Figure 11 Comparison of sorption and dilation isotherms for PSU/CO_2/35°C (parameters of the fitted interpolation function: $b = 5.77$; $c = 0.475$)

Dilation isotherms

Poly(sulfone). For poly(sulfone)/CO_2 the two dilation isotherms are compared with the sorption isotherm in *Figure 11*. It can be seen that the primary dilation follows directly the gas concentration while the long-time dilation curve exhibits significant deviations in the pressure range above 15 bar. The difference between the two dilation isotherms represents the secondary volume relaxation. A similar behaviour is found for nitrous oxide in PSU (*Figure 12*) where the secondary dilation comes into effect at lower gas pressures and is more pronounced at higher gas pressures.

In contrast, the secondary volume relaxation can be neglected over the whole pressure range for methane in PSU at a significantly lower concentration level (*Figure 13*). The corresponding plot of ($\Delta V/V_0$) against gas concentration C with straight lines approximately representing the limiting slopes of the curve (*Figure 14*) results in a decreasing partial molar volume (PMV) ranging from 17.5 to 14.1 cm^3/mol in the pressure range under investigation.

For carbon dioxide and nitrous oxide exhibiting higher gas concentrations and therefore stronger gas/polymer interactions the volumetric behaviour of the polymer matrix can be compared on the basis of the concentration-dependent volume change in *Figures 15 and 16*. Both gas molecules are isoelectronic and isosteric but the N_2O-molecules possess a dipole moment of about 0.17 D[24] due to their asymmetric structure. The size of the molecules is also very similar, as can be seen from the Lennard–Jones parameter σ which is $3.941 \cdot 10^{-10}$ m and $3.828 \cdot 10^{-10}$ m for CO_2 and N_2O, respectively[25], and the kinetic collision diameter σ_{kin} of $3.3 \cdot 10^{-10}$ m for both gases, calculated from the minimum cross-sectional diameter of the molecule[26]. σ_{kin} is often used for the discussion of transport and adsorption properties of gases.

Comparing the curves of the short-time analysis for CO_2 and N_2O one can clearly see similarities in the volumetric

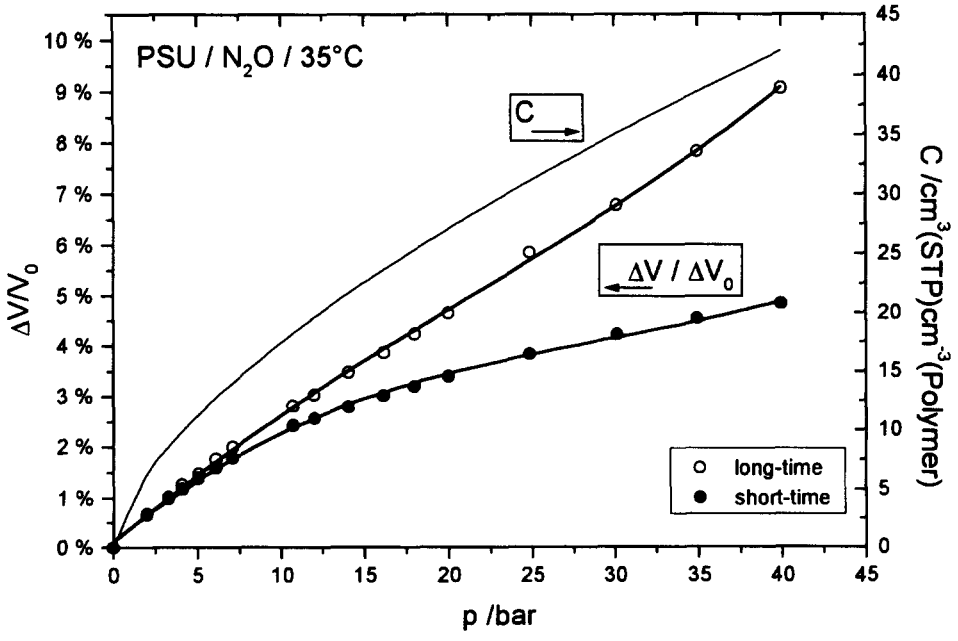

Figure 12 Sorption and dilation isotherms—PSU/N_2O/35°C (parameters of the fitted interpolation function: $b = 4.07$; $c = 0.633$)

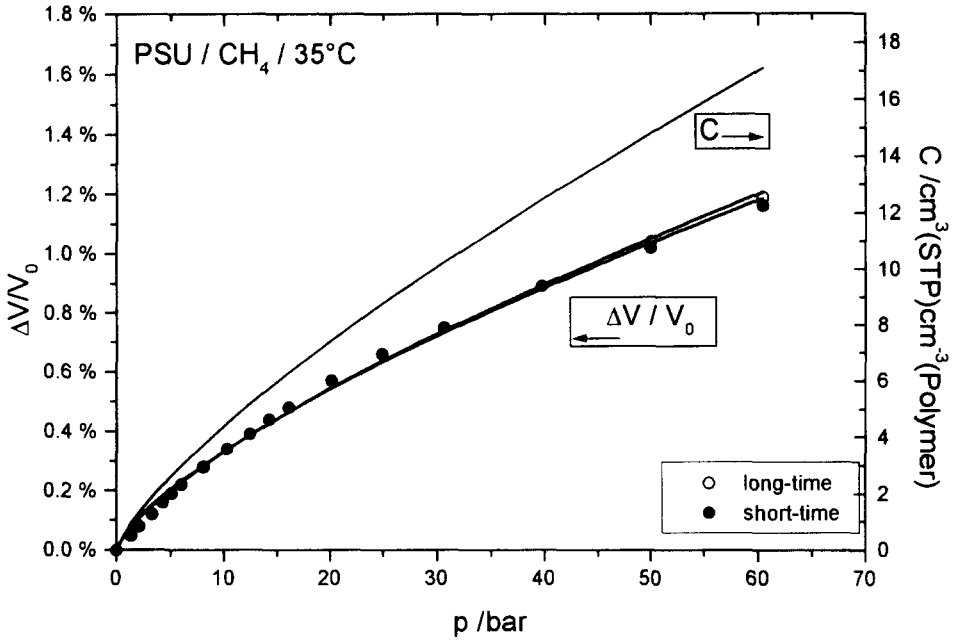

Figure 13 Sorption and dilation isotherms—PSU/CH_4/35°C (parameters of the fitted interpolation function: $b = 0.779$; $c = 0.754$)

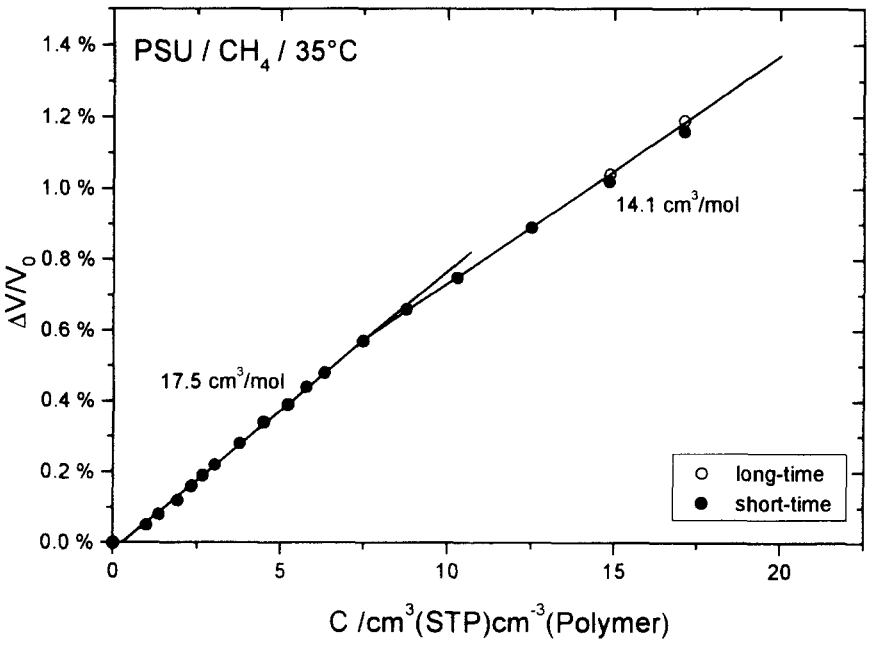

Figure 14 Concentration-dependent volume change and PMV–PSU/CH_4/35°C

behaviour. The transition between the two almost linear parts of the short-time curve occurs at lower gas concentrations for N_2O. The PMV resulting from the low-concentration part of the curve is somewhat higher for CO_2, while after the transition nearly the same PMV of about 23 cm^3/mol is observed for both gases (*Table 2*). For N_2O also the enhanced volume relaxation comes into effect at significantly lower concentrations. The comparison of the volume change at $C = 35$ cm^3(STP)/cm^3(polymer), i.e. above the transition to the distinct volume relaxation behaviour, shows for PSU/CO_2 a short-time volume change of $(\Delta V/V_0)_{1,C=35} = 4.77\%$ and the long-time analysis results in $(\Delta V/V_0)_{2,C=35} = 6.93\%$. For PSU/$N_2O$ one finds volume changes of $(\Delta V/V_0)_{1,C=35} = 4.18\%$ and $(\Delta V/V_0)_{2,C=35} = 6.92\%$ being very close to the corresponding values for CO_2. The influence of the sorbed gas molecules on the volume of the polymer matrix therefore seems to be very similar. The appearance of the volume relaxation processes at lower concentrations for N_2O reveals the higher polymer chain mobility compared with the PSU/CO_2-system. This stronger plasticisation effect may be attributed to the polar character of nitrous oxide, i.e. the dipole moment of the gas molecules, resulting in stronger gas/polymer interactions. The initiation of the pronounced volume relaxation behaviour, i.e. reaching a sufficient chain mobility for the relaxation process to occur, at higher gas concentrations for CO_2 leads, in consequence, to a higher apparent PMV approaching the same level of volume change at about 35 cm^3(STP)/cm^3(polymer).

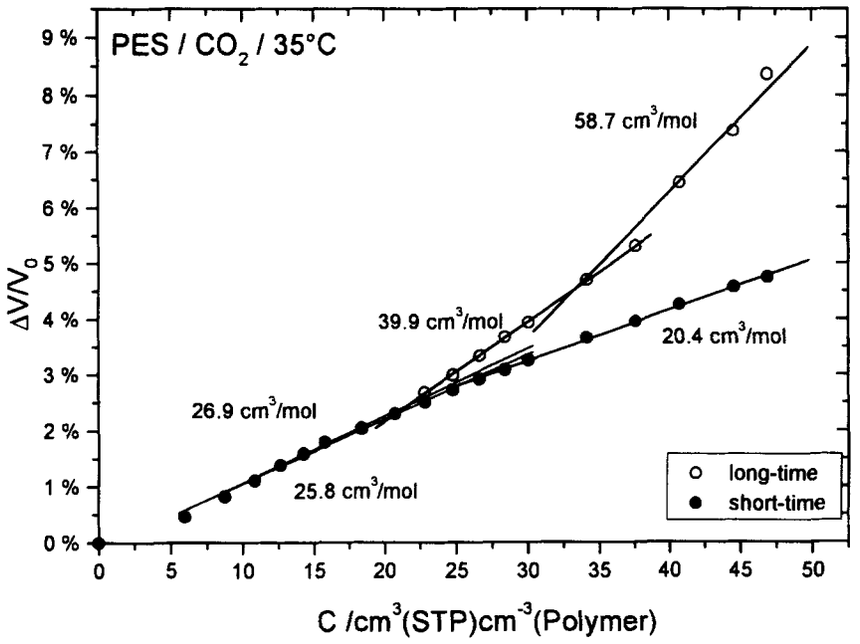

Figure 15 Concentration-dependent volume change and PMV–PSU/CO_2/35°C

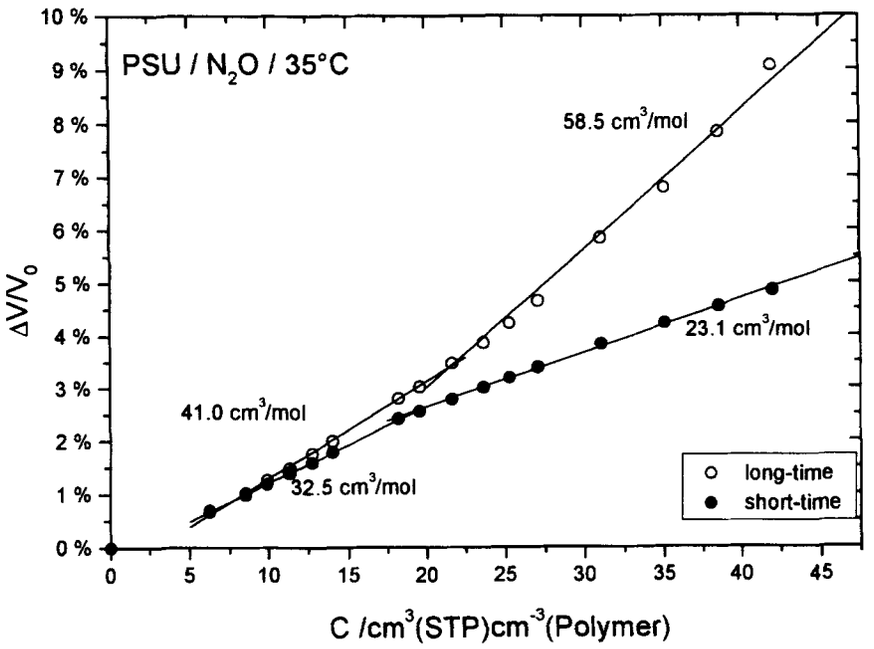

Figure 16 Concentration-dependent volume change and PMV–PSU/N_2O/35°C

Table 2 Partial molar volumes for all polymer/gas systems investigated in this study calculated from the slopes of the concentration-dependent volume change

Gas	Polymer	PMV/cm³ mol⁻¹	
CO_2	PSU	39.9–23.5	short-time
		43.7–65.0	long-time
CO_2	PES	25.8–20.4	short-time
		26.9–58.7	long-time
N_2O	PSU	32.5–23.1	short-time
		41.0–58.5	long-time
N_2O	PES	27.6	short-time
		31.6–63.8	long-time
CH_4	PSU	17.5–14.1	short-time
		-/-	long-time
CH_4	PES	15.7	short-time
		-/-	long-time

Poly(ether sulfone). Sorption and dilation isotherms for PES are, in general, equivalent to those observed for PSU. Again the dilation isotherms essentially follow the course of the sorption isotherms. For carbon dioxide (*Figure 17*) and nitrous oxide (*Figure 18*) a distinct volume relaxation is found above 10 bar and at approximately 7 bar, respectively, while for methane no secondary volume change could be observed (*Figure 19*). As a result PES/methane shows a linear volume increase with increasing gas concentration and a constant PMV of 15.7 cm³/mol (*Figure 20*).

The gases exhibiting higher solubilities in the polymer, CO_2 and N_2O, can be compared as described above for PSU. The concentration dependent volume change is shown in *Figure 21* and *Figure 22*. For both gases an almost constant PMV results from the short-time analysis: 25.8 cm³/mol

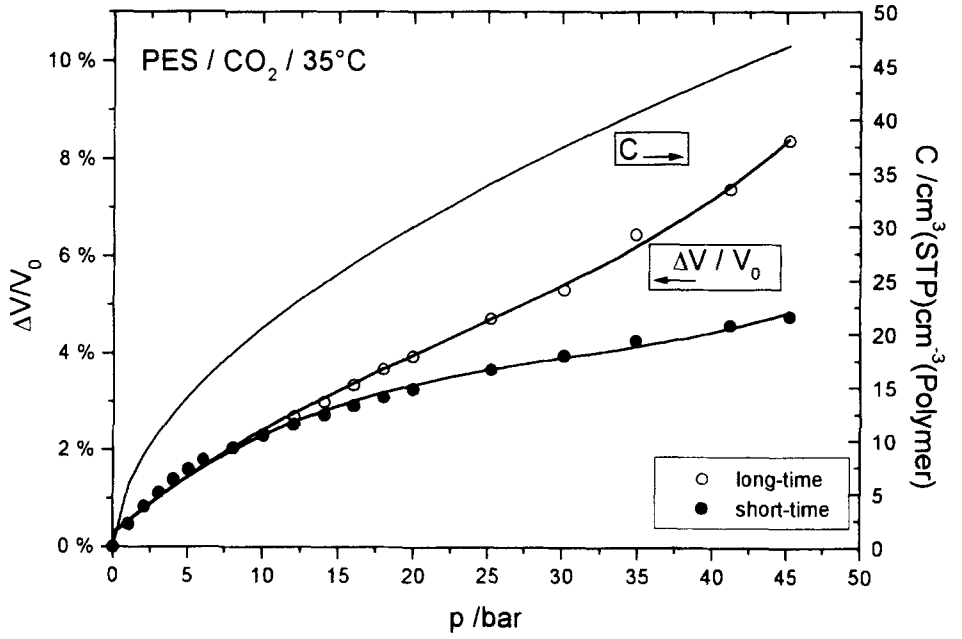

Figure 17 Sorption and dilation isotherms—PES/CO_2/35°C (parameters of the fitted interpolation function: $b = 5.90$; $c = 0.544$)

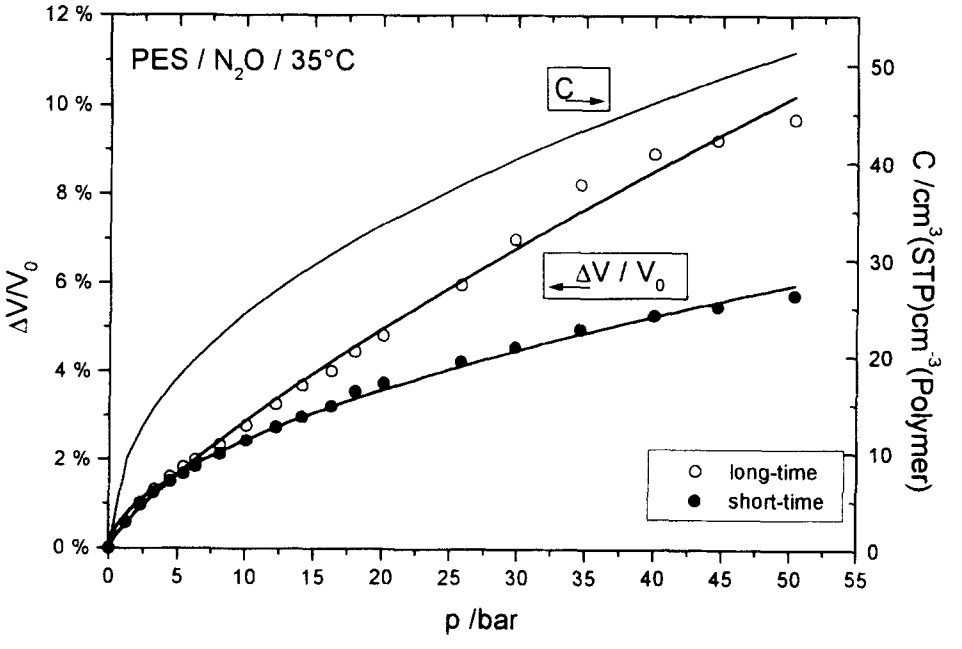

Figure 18 Sorption and dilation isotherms—PES/N_2O/35°C (parameters of the fitted interpolation function: $b = 8.49$; $c = 0.460$)

decreasing with increasing C to 20.4 cm^3/mol (CO_2) and 27.6 cm^3/mol (N_2O). For PES/CO_2 not a single sharp transition to the pronounced volume relaxation behaviour is observed. The initially only gradually increasing volume change is represented in *Figure 21* by an intermediate region between 20 and 32 cm^3(STP)/cm^3(polymer). Generally, for PES/N_2O the volume relaxation comes into effect at lower concentrations in comparison with PES/CO_2, indicating a stronger plasticisation effect due to gas/polymer interactions for N_2O as already stated for PSU.

The volume changes found slightly above the transition to the distinct volume relaxation at approx. 30 cm^3(STP)/cm^3(polymer) for both polymer/gas-systems again indicate similar volumetric influences of the two gases on the polymer matrix. The observed volume changes for short-time (index 1) and long-time analysis (index 2) at this concentration level are for PES/CO_2

$$\left(\frac{\Delta V}{V_0}\right)_{1,C=30} = 3.27\% \text{ and } \left(\frac{\Delta V}{V_0}\right)_{2,C=30} = 3.95\%$$

and for PES/N_2O

$$\left(\frac{\Delta V}{V_0}\right)_{1,C=30} = 3.15\% \text{ and } \left(\frac{\Delta V}{V_0}\right)_{2,C=30} = 4.00\%$$

Reversibility of dilation processes

To reverse the dilation process of the polymer matrix the sample has to be totally degassed to release the internal stresses exerted by the sorbed gas molecules being the cause of swelling phenomena. The volume relaxation observed as a secondary process in dilation experiments depends on

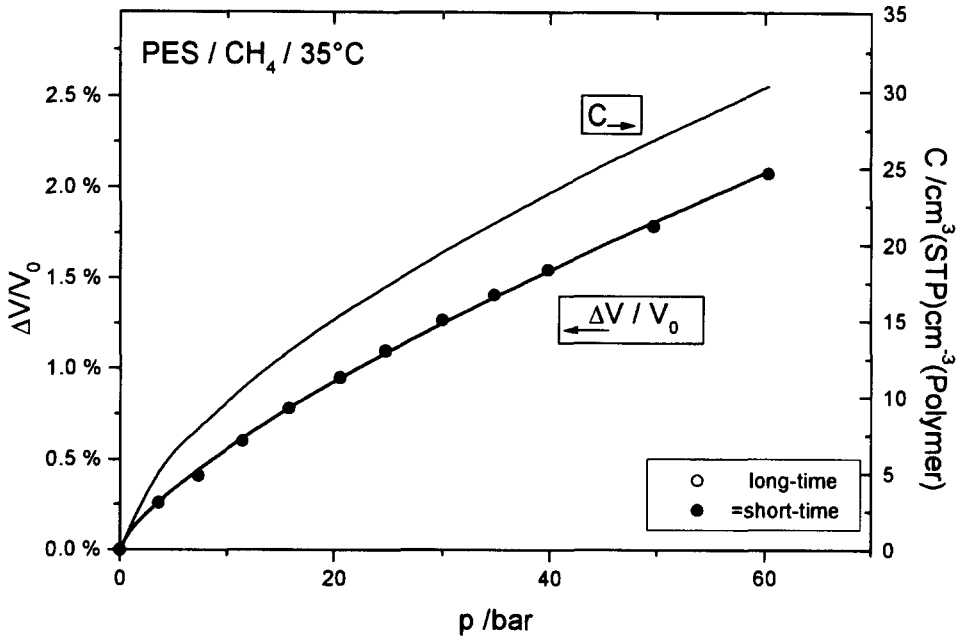

Figure 19 Sorption and dilation isotherms—PES/CH_4/35°C (parameters of the fitted interpolation function: $b = 2.27$; $c = 0.633$)

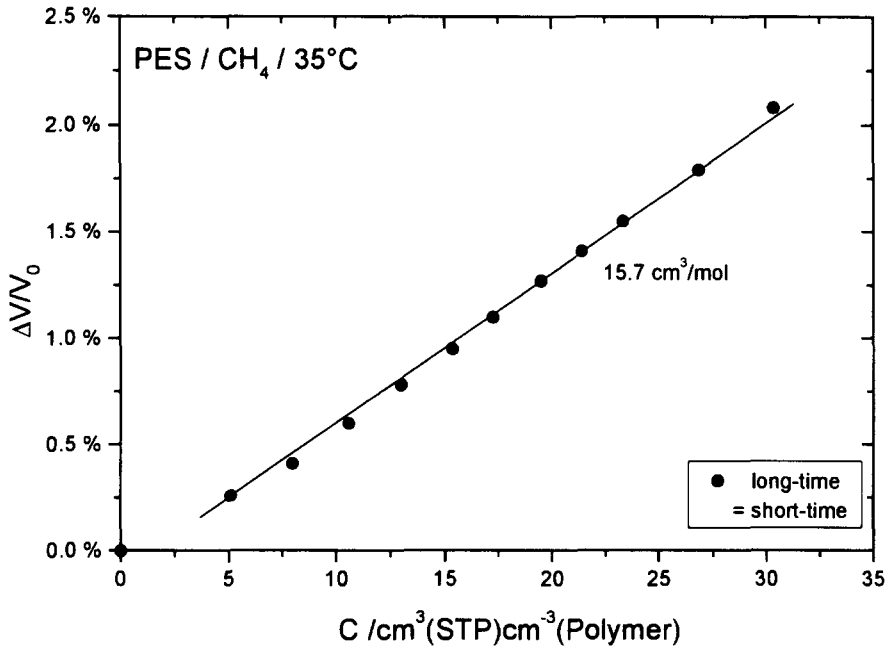

Figure 20 Concentration-dependent volume change and PMV–PES/CH_4/35°C

sufficient mobility of the polymer chains influenced by the gas concentration within the polymer sample. The stepwise pressurisation during the course of experimental determination of dilation isotherms leads to an increasing amount of gas molecules present in the polymer and therefore an increasing chain mobility as a result of plasticisation. Hence, the depressurisation leads to a decrease of polymer chain mobility due to decreasing gas concentrations.

For the secondary relaxational dilation process to be completely reversible, the same polymer chain mobility would be required during depressurisation, as it was in effect during pressurisation. Only an infinitely slow depressurisation process would meet this precondition which is practically unfeasible.

On the other hand, irreversible changes of the polymer's microstructure, usually referred to as conditioning, could be expected since the glassy state does not represent a thermodynamic equilibrium. Minor internal stresses and inhomogeneities frozen in during the preparation of the polymer samples must always be taken into account for melt-extruded as well as for solution-cast films.

An attempt to characterise the reversible dilation behaviour has been made by means of two successive one-step dilation experiments raising the pressure immediately from vacuum to 50 bar (after initial degassing of the sample) and after measuring the changing sample length for 24 to 48 h, releasing the pressure within *ca.* 15 min and degassing for another 24–48 h under vacuum conditions. In *Figure 23* the corrected distance curves for PSU/CO_2 at 35°C are shown as an example.

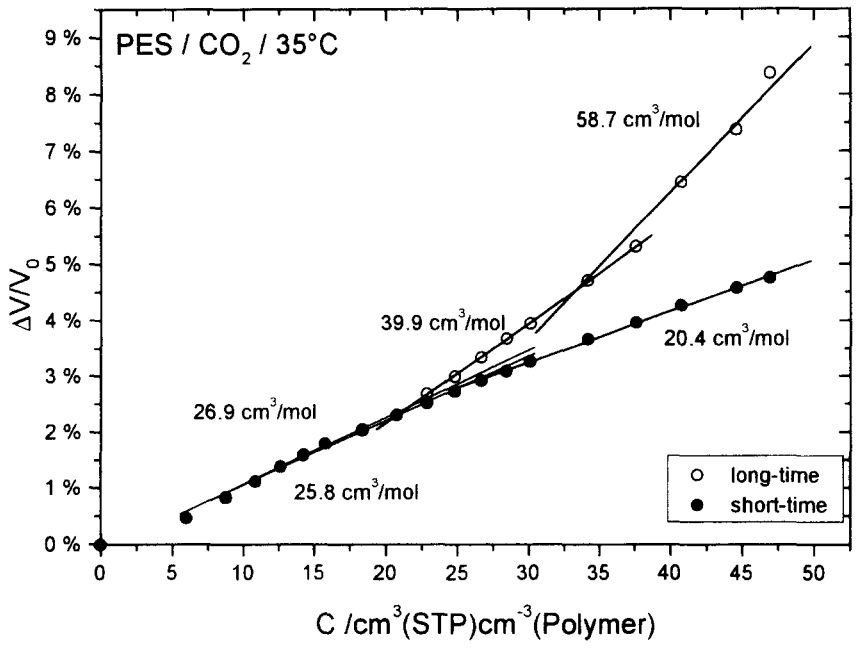

Figure 21 Concentration-dependent volume change and PMV–PES/CO_2/35°C

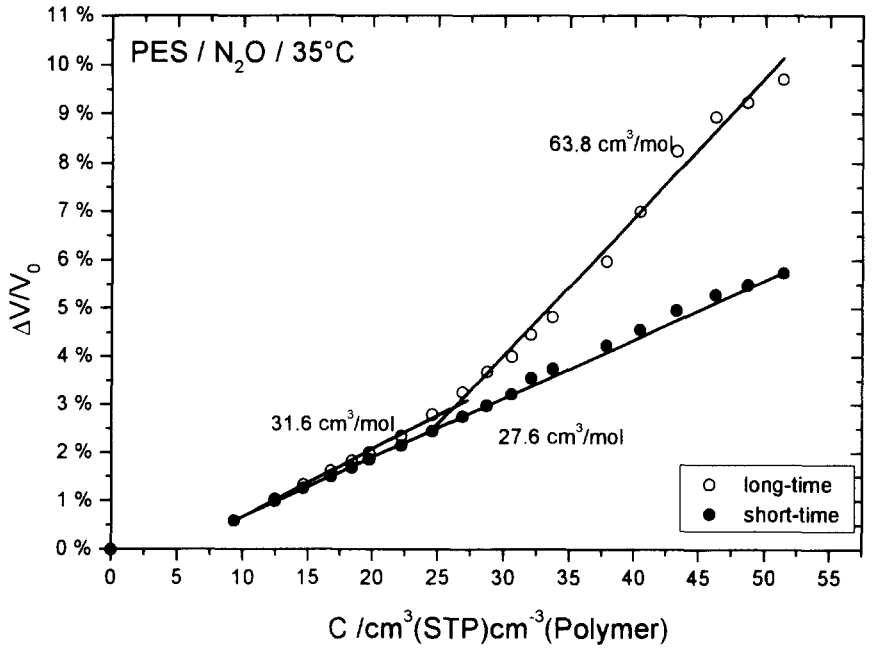

Figure 22 Concentration-dependent volume change and PMV–PES/N_2O/35°C

The degassing after a maximum length change of 2.09% ($\Delta d = 0.416$ mm) results in a decrease of the sample length ($l_0 = 19.880$ mm) by 0.09% ($\Delta l = -0.017$ mm). During the second one-step experiment a maximum length change of 2.26% and another contraction of the sample by 0.16% ($\Delta l = -0.031$ mm) was observed for the polymer film preconditioned in the first dilation step. Minor differences compared with the maximum length-dilation found during the corresponding multi-step experiment are due to different boundary conditions and the different time-scale of the one-step measurement. The contraction of the sample must be attributed to the relaxation of internal stresses enabled by the enhanced polymer chain mobility due to the plasticising effect of sorbed CO_2. This conditioning process leads to a slightly altered dilation behaviour and a further contraction of the film sample. On the basis of these results deviations due to conditioning can be roughly estimated to be within 10% of the observed dilation effects.

The occurrence of contraction phenomena after dilation experiments also supports the assumption that significant creep processes within the samples can be neglected for the experimental set-up and time-scales used in this study.

For all dilation isotherms presented here a consolidation of at least 90% was observed after degassing, i.e. the measured final distance was >90% of the initial distance prior to the swelling of the sample.

CONCLUSIONS

The experimental set-up for gas-pressure dilatometric

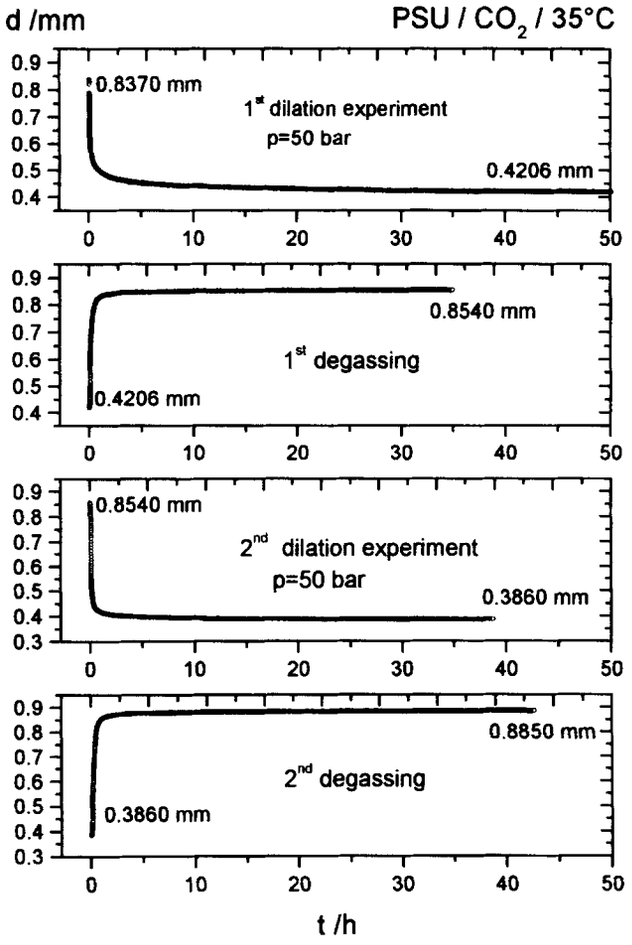

Figure 23 Successive one-step dilation experiments—PSU/CO_2/35°C

experiments with polymer films based on capacitive distance measurements provides an easily automated way to investigate the volumetric behaviour of polymers under elevated gas pressures. The analysis of different time ranges of the individual dilation steps makes a separate examination of the diffusion-related sorptive dilation and the secondary relaxational dilation process possible.

For all polymer/gas systems investigated in this study the dilation isotherms generally follow the course of gas sorption. The increasing relaxational dilation represents the enhanced chain mobility within the polymer matrix due to the plasticising effect of the sorbed gas molecules.

REFERENCES

1. Koros, W. J. (ed.), *ACS Symp. Ser.*, **1990**, 423.
2. Koros, W. J. and Fleming, G. K., *J. Membrane Sci.*, 1993, **83**, 1.
3. Prasad, R., Notaro, F. and Thompson, D. R., *J. Membrane Sci.*, 1994, **94**, 225.
4. Paul, D. R. and Yampol'skii, Y. P. (eds.) in *Polymeric Gas Separation Membranes*. CRC Press, Boca Raton, LA, 1994.
5. Kesting, R. E. and Fritzsche, A. K., *Polymeric Gas Separation Membranes*. Wiley, New York, 1993.
6. Frisch, H. L. and Stern, S. A., *CRC Crit. Rev. Solid State Mat. Sci.*, 1983, **11**, 123.
7. Paul, D. R., *Ber. Bunsenges. Phys. Chem.*, 1979, **83**, 294.
8. Kamiya, Y., Hirose, T., Mizoguchi, K. and Naito, Y., *J. Polym. Sci. Part B: Polym. Phys.*, 1986, **24**, 1525.
9. Kirchheim, R., *Macromolecules*, 1992, **25**, 6952.
10. Raucher, D. and Sefcik, M. D., in *Industrial Gas Separations. ACS Symp. Ser.*, 1983, **223**, 111.
11. Bitter, J. G. A., *Transport Mechanisms in Membrane Separation Processes*. Plenum Press, New York, 1991.
12. Sefcik, M. D., *J. Polym. Sci. Part B: Polym Phys.*, 1986, **24**, 957.
13. Fleming, G. K. and Koros, W. J., *Macromolecules*, 1986, **19**, 2285.
14. Hirose, T., Mizoguchi, K. and Kamiya, Y. *J. Polym. Sci. Part B: Polym. Phys.*, 1986, **24**, 2107.
15. Wissinger, R. G. and Paulaitis, M. E., *J. Polym. Sci. Part B: Polym. Phys.*, 1987, **25**, 2497.
16. Pope, D. S., Koros, W. J. and Fleming, G. K., *J. Polym. Sci. Part B: Polym. Phys.*, 1989, **27**, 1173.
17. Briscoe, B. J. and Zakaria, S., *J. Polym. Sci. Part B: Polym. Phys.*, 1991, **29**, 989.
18. Wessling, M., Huismann, I., van den Boomgard, T. and Smolders, C. A., *J. Polym. Sci Part B: Polym. Phys.*, 1995, **33**, 1371.
19. Kamiya, Y., Hirose, T., Naito, Y. and Mizoguchi, K., *J. Polym. Sci. Part B: Polym. Phys.*, 1988, **26**, 159.
20. Schultze, J.D., Zhou, Z. and Springer, J., *Angew. Makromol Chem.*,, 1991, **185/186**, 3279.
21. System Manual, capa-NCDT, Micro-Epsilon Meßtechnik, Ortenburg, Germany, 1990.
22. Crank, J., *The Mathematics of Diffusion*, 2nd ed. Oxford University Press, Oxford, 1975.
23. Xu, Z.-K., Böhning, M., Springer, J., Steinhauser, N. and Mülhaupt, R., *Polymer*, 1997, **38**, 581.
24. Greenwood, N. N. and Earnshaw, A., *Chemistry of the Elements*, 1st ed. Pergamon Press, Oxford, 1984.
25. Reid, R. C., Prausnitz, J. M. and Poling, B. E., *The Properties of Gases and Liquids*. McGraw-Hill, New York, 1988.
26. Breck, D. W., *Zeolite Molecular Sieves—Structure, Chemistry and Use*. Wiley, New York, 1974.